Arabian Journal of Chemistry (2016) 9, 350–356

King Saud University

Arabian Journal of Chemistry

www.ksu.edu.sa
www.sciencedirect.com

ORIGINAL ARTICLE

Electrochemical behaviour of antioxidants: Part 2. Electrochemical oxidation mechanism of quercetin at glassy carbon electrode modified with multi-wall carbon nanotubes

Refat Abdel-Hamid *, **Mostafa K. Rabia, Emad F. Newair**

Department of Chemistry, Faculty of Science, University of Sohag, 82524 Sohag, Egypt

Received 28 March 2012; accepted 12 June 2012
Available online 4 August 2012

KEYWORDS

Quercetin;
Cyclic voltammetry;
Chronocoulometry;
Digital simulation

Abstract Electrochemical oxidation mechanism of quercetin was investigated at glassy carbon electrode modified with multi-wall carbon nanotubes in aqueous 0.2 M phosphate solutions with different pHs. The investigation was carried out using cyclic voltammetry, double potential step chronoamperometric and chronocoulometric techniques. It was found that the oxidation mechanism proceeds in sequential steps, related with the five-hydroxyl groups in the three aromatic rings. The mechanism was proposed to be an ECEC, first-order kinetics. The proposed mechanism was confirmed on comparing the digital simulated cyclic voltammetric responses with the experimental ones. The electrode homogeneous and heterogeneous kinetic parameters of electrode reaction are estimated from the simulated data. Moreover, quercetin molecules adsorb on the electrode surface.

1. Introduction

Flavonoids represent a large group of polyphenol secondary metabolites that are widely distributed in medicinal plants, fruits, teas and health beverages (Manach et al., 2004). Quercetin, Qu, a derivative of benzo-γ-pyrone, is a bioflavonoid. Bioflavonoids are a large family of naturally occurring organic compounds widely distributed in plants. Bioflavonoids are highly interesting because they may exert a wide range of beneficial effects on human health and have broad pharmacological activities including prevention of cardiovascular diseases and different forms of cancer. Quercetin (3, 3′, 4′, 5, 7-pentahydroxyflavone) is predominant in vegetables and fruits. It is a penta-hydroxyl antioxidant (Mora et al., 1990 and van Acker et al., 1996). Electrochemical oxidation of quercetin was studied at glassy carbon (Pierozynski and Zielinska, 2011; Zielinska et al., 2010; Medvidović-Kosanović et al., 2010; Zielinska and Pierozynski, 2009; Simić et al. 2007; Timbola et al., 2006; Zare et al., 2005; Nematollahi and Malakzadeh, 2003; Brett and Ghica, 2003), platinum (Mase et al., 2011; Brett and Ghica, 2003), polycrystalline platinum (Pierozynski and Zielinska, 2010),

* Corresponding author.
E-mail addresses: abdelhamid_refat@yahoo.com (R. Abdel-Hamid), mostafarabia@hotmail.com (M.K. Rabia), newer_emad84@yahoo.com (E.F. Newair).
Peer review under responsibility of King Saud University.

ELSEVIER Production and hosting by Elsevier

1878-5352 © 2013 Production and hosting by Elsevier B.V. on behalf of King Saud University.
http://dx.doi.org/10.1016/j.arabjc.2012.06.014

multi-wall carbon nanotubes (Gutiérrez et al., 2010), paraffin-impregnated graphite disk modified with multi-wall carbon nanotubes (Jin et al., 2006), plastic formed carbon (Yang et al., 2001), procaine and aminophenyl modified (Mulazimoglu and Ozkan 2008) and graphite-wax electrodes (He et al., 2009). The products of quercetin electrochemical oxidation adsorb on glassy carbon electrode surface (Medvidović-Kosanović et al., 2010). The initial step is oxidation of quercetin's two –OH catechol groups in ring B. The following steps are oxidation of the remaining three hydroxyl groups, located in rings C and A. Gutiérrez et al. (Gutiérrez et al., 2010), reported that, in the presence of carbon nanotubes, the oxidation and reduction currents of the less positive wave increase while the peak potential separations almost do not change. The enhancement in the currents is due to the increase of the electroactive area of the modified electrode surface.

Earlier authors reported that, the electrochemical oxidation of quercetin proceeds via two steps. Each step involves transfer of one electron and one proton, to give *semi*quinone and finally the *ortho*quinone. No electrochemical parameters were estimated. Furthermore, little attention has been paid to its electrochemical oxidation mechanism on carbon nanotubes, CNTs. However, in continuation of our work on electrochemical behaviour of antioxidants (Abdel-Hamid and Newair, 2011), in this work, a glassy carbon electrode modified with multi-wall carbon nanotubes was prepared and used to study the electrochemical behaviour of quercetin. The electrochemical oxidation mechanism is investigated, using cyclic voltammetry, double potential step chronoamperometry and chronocoulometry and digital simulation. The electrochemical oxidation mechanism of quercetin is proposed and discussed. The proposed mechanism was confirmed using digital simulation and the electrochemical parameters are estimated. This may play a crucial role in understanding its antioxidant activity. The study is performed in aqueous phosphate solutions on modified electrode.

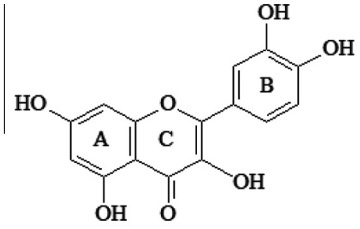

The chemical structure of quercetin

2. Materials and methods

All the electrochemical experiments were carried out using Model 273A potentiostat from EG & G Princeton Applied Research equipped with EG & G M 270 software. The working electrode was glassy carbon/multi-wall carbon nanotubes modified electrode, GCE/MWCNTs. 1.0 mg/mL suspension of MWCNTs was obtained on dispersing five milligrams of MWCNTs in 5.0 cm^3 N,N-dimethylformamide (DMF). The mixed solution was ultrasonically agitated for 6 h. The GCE/MWCNTs, modified electrode was prepared by adding a drop of 1.0 cm^3 of MWCNTs suspension (1.0 mg cm^{-3}) onto the clean surface of GCE. Then the solvent was evaporated overnight. The glassy carbon electrode was polished with 0.5 μm alumina powder on a polishing cloth to obtain a mirror-like surface before modification. After rinsing the surface with deionized water, the polished GCE was sonicated for 5 min in water/ethanol to get rid of the trace amount of alumina powder from the surface and rinsed again with deionized water. Then, the surface was fully dried at atmospheric condition with a stream of purified nitrogen. A platinum electrode and a saturated calomel electrode (SCE) were used as the counter and reference electrodes, respectively. All the potentials were reported with respect to this reference electrode. All experiments were performed at room (25 °C) temperature.

All the chemical reagents used for solutions were of reagent grade from Merck and used as received. The MWCNTs (purity: >90%; carbon basis, D × L 110–170 nm × 5–9 μm) were from Aldrich. All solutions were freshly prepared just before use with deionized water. The uncompensated resistance was corrected by the potentiostat.

3. Results and discussion

3.1. Cyclic voltammetry

The electrochemical behaviour of quercetin, at a glassy carbon electrode modified with multi-wall carbon nanotubes is investigated in 0.2 M phosphate aqueous buffer solutions at different pHs. Fig. 1A shows the cyclic voltammograms, cv, of 2.5 μM quercetin in buffer solution (pH 2.12) at scan rate of 10 mV/s. The overall cyclic voltammogram, cv Fig. 1A, shows four anodic peaks associated with the oxidation centres present in the Qu molecule occurring at potentials of 0.47, 0.56, 0.84 and 1.13 volts. The cv profile is similar to those previously reported (Brett and Ghica, 2003).

The first anodic cv wave, located at ≈0.47 volts, seems to be reversible, its cathodic counter-part is seen, on reversing the potential scan just before the second wave, c.f. Fig. 1B. The peak separation between the anodic peak potential, E_{pa}, and the cathodic peak potential, E_{pc}, $\Delta E_p = E_{pa} - E_{pc}$, is ≈40 mV which agrees with literature data which points to a reversible electrode reaction involving two electrons (Bard and Faulkner, 2001). The somewhat high peak separation value could point to a slow electron-transfer or chemical contribution. On increasing scan rate, E_{pa} is positively shifted and the E_{pc} is negatively shifted. The relationship of anodic peak potential with scan rate indicates that the electron-transfer process couples with a chemical reaction. On plotting peak currents, i_{pa} and i_{pc} as a function of scan rate square root ($v^{1/2}$), a linear relation is obtained with correlation coefficients, r, 0.985. This indicates that the oxidation process of Qu is diffusion-controlled. These findings point out to a diffusion-controlled electrode process involving a follow-up chemical reaction to the electron transfer process (Bard and Faulkner, 2001).

The oxidation products formed in the first peak are electrochemically active, which further oxidize at higher potentials, giving the second cv wave, located at ≈0.56 volt. On reversing the potential scan just before the third wave, a reduction wave appears at about 0.44 V, c.f. Fig. 1C. This wave is the counter-part of first oxidation cv wave. Thus, the second oxidation cv wave is irreversible, its counter-part is not seen. On increasing scan rate, peak potential, E_{pa}, of the second wave is shifted to more posi-

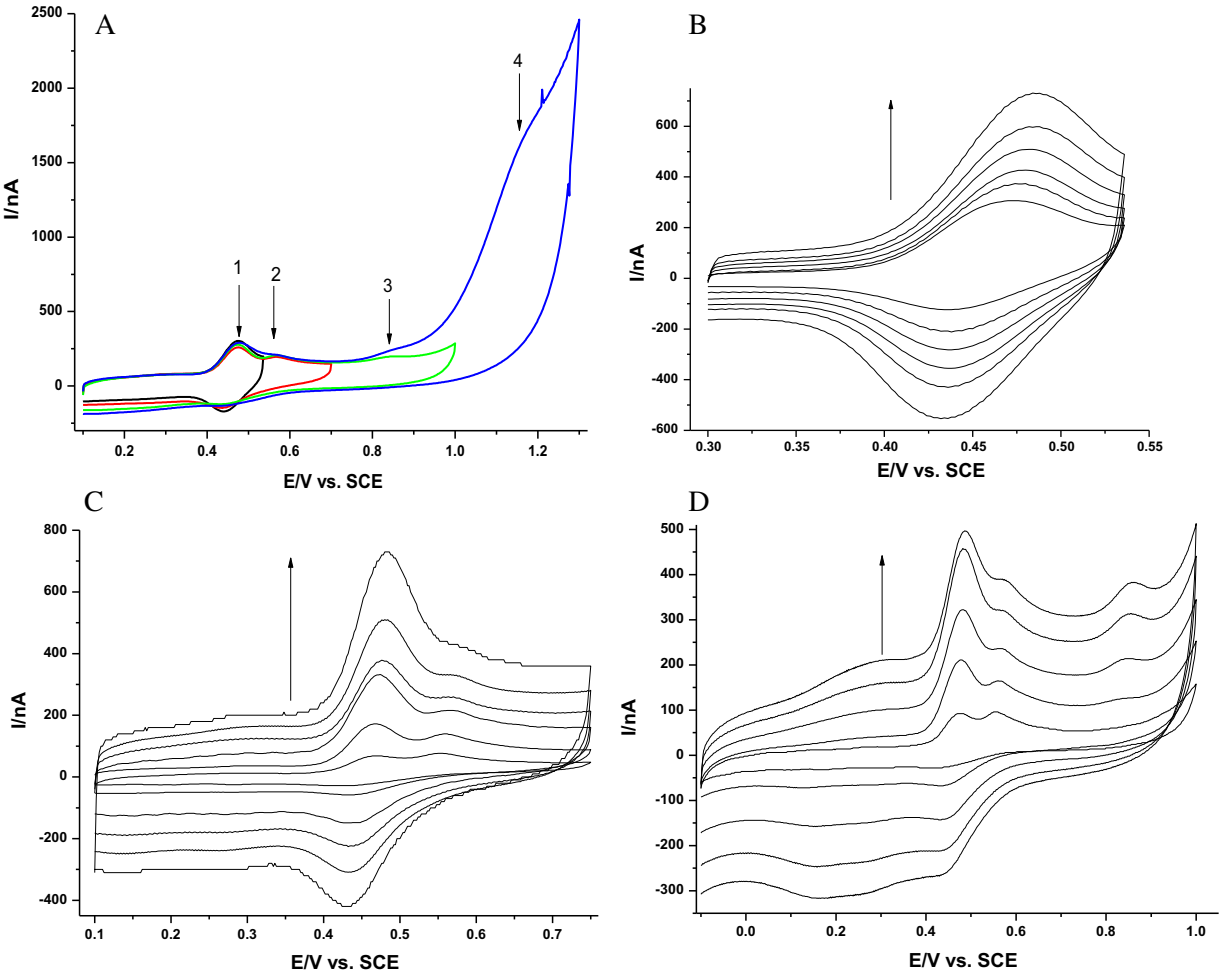

Figure 1 (A).Cyclic voltammograms of 2.5 μM Quercetin in 0.2 M pH 2.12 phosphate buffer at scan rate of 10 mV/s at different switching potentials, (B). is for the 1st wave at different scan rates (10, 15, 20, 25, 30, 40 mV/s), (C) for the 1st and 2nd waves at different scan rates (5, 10, 20, 30, 40 mV/s), (D) for the 1st, 2nd and 3rd waves at different scan rates (5, 10, 20 mV/s).

tive value. This indicates that the electron transfer process has a slow electron transfer rate or coupled with a homogenous chemical reaction. Relatively low peak current of second cv wave is attributed to the formation of intermolecular hydrogen bond between the 3-hydroxyl group and the close oxygen at position 4 at ring C. The second wave is related to a reaction which involves the next hydroxyl group, 3-hydroxy group on ring C (Zielinska et al., 2010). A linear dependence of the peak current, i_{pa}, on scan rate is obtained with correlation coefficients of 0.942. This reveals that, the rate of oxidation of quercetin along the second wave is mainly controlled by adsorption and corresponds to further redox of the adsorbed intermediates (He et al., 2009).

On extending the potential window to 1.0 V, just before the fourth cv wave, the oxidation products formed at the second wave is further oxidized at about 0.85 V, giving rise to the third cv wave and next other waves. On switching the potential scan, two cathodic waves are seen at about 0.44 and 0.16 V, c.f. Fig. 1D. The first is related to the first oxidation wave, while the other wave corresponds to the third one. Their wide appearance reveals the complexity of the formed oxidation products (He et al., 2009). This wave is attributed to the oxidation of the hydroxyl group attached at the 5-position of A-ring (Brett and Ghica, 2003). Its peak current, i_{pa}, varies with scan rate linearly with a correlation coefficient of 0.997. This indicates that, the rate of oxidation of quercetin along this cv waves is controlled mainly by adsorption.

On sweeping potential to more positive values, up to 1.3 V, fourth oxidation cv wave is obtained at about 1.13 V. On switching the potential scan, two cathodic waves are seen at about 0.44 and 0.16 V. They are related to the first oxidation wave and the other ones (He et al., 2009). The fourth oxidation cv wave is due to the oxidation of the 7-hydroxyl group of A-ring (Brett and Ghica, 2003). A linear variation of peak current as a function of scan rate relation, is obtained with correlation coefficients of 0.979, indicating that, the rate of oxidation of quercetin along this cv wave is controlled by adsorption.

The final products of these oxidations adsorb strongly on electrode surface. This adsorption reduces the anodic response of the first and second cv waves on multiple cyclic scanning, c.f. Fig. 2A. After scanning the cv of quercetin solution, a linear sweep voltammogram, LSV, is recorded for the working electrode in a cell containing only the supporting electrolyte.

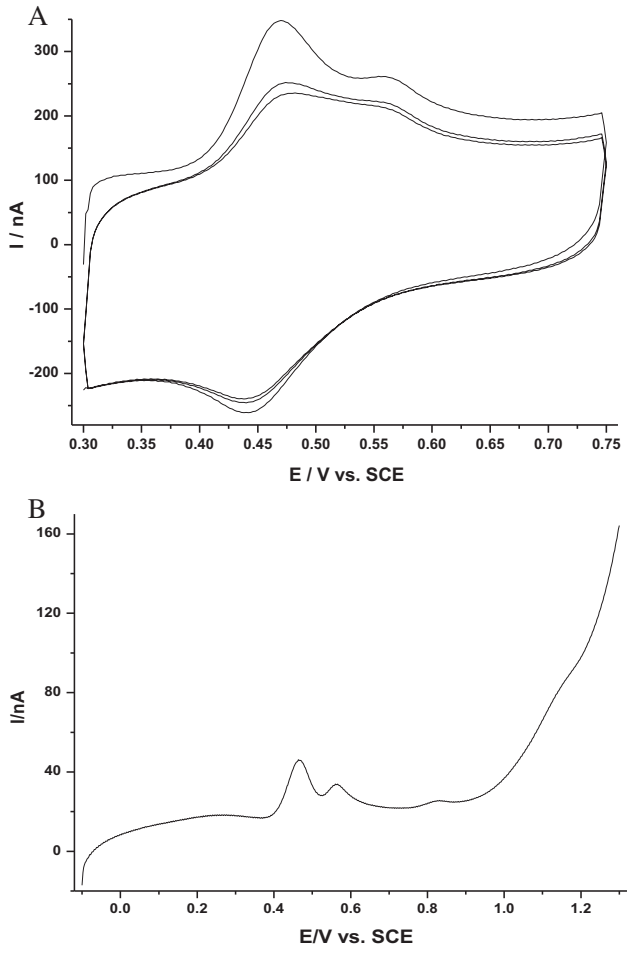

Figure 2 Voltammograms of 2.5 μM Quercetin in 0.2 M phosphate buffer at pH 2.12: (A) Multicyclic voltammograms at scan rate 30 mV/s for 3 cycles, (B) Linear scan voltammogram, LSV, recorded for the electrode in a cell containing only the supporting electrolyte.

Fig. 2B represents the obtained LSV. This supports the adsorption of quercetin on the working electrode surface.

On increasing the pH of solution, a variation of the electrochemical response of 2.5 μM Qu is observed. The main response observed for most pHs is for the first and second cv waves, whereas the third and fourth ones occur only as shoulders. At higher pHs (>6.75) quercetin is associated with decomposition. Therefore, quercetin has the highest stability at lower pHs (⩽6.75). This stability is attributed to the fully protonated Qu molecules at such conditions (Álvarez-Diduk et al., 2009). On increasing the pH of solution, the anodic peak currents, i_{pa}, decrease and the peak potentials, E_{pa}, shift to less positive direction for the first and second cv waves, respectively. This is ascribed to the expected proton participation in the oxidation reaction. Linear least squares relationships between E_{pa} and pH value for the two waves are obtained. The slopes are ≈−69 mV/pH. These slopes are close to the theoretical value at 298 K, corresponding to a mechanism, which involves the transfer of the same number of electrons and protons. According to EC mechanism, the oxidation of Qu involves the participation of one-electron and one-proton that leads to the formation of *semi*quinone, which can be further oxidized in a one-electron and one-proton forming *ortho*-quinone.

3.2. Double potential step chronoamperometry

Double potential step chronoamperometry is used for the determination of diffusion coefficient and deduce the current nature. The chronoamperograms of 2.5 μM quercetin in 0.2 M phosphate buffer solution (pH 2.12) are obtained at different duration times. The current of the first step, $i(t < \tau)$, is unaffected by the chemical reaction, so that it is used to estimate the diffusion coefficient. The diffusion coefficient is estimated on applying the Cottrell's equation (Bard and Faulkner, 2001):

$$i(t > \tau) = n\mathrm{FAD}^{1/2}\ \mathrm{C}^{*}_{\mathrm{bulk}}\pi^{-1/2}t^{-1/2} \tag{1}$$

where D is the diffusion coefficient ($cm^2\ s^{-1}$), C^{*}_{bulk} is bulk concentration (mol/cm^3), τ is the step duration time, and n, F and A have their usual significance. In a particular chronoamperometric experiment, the electrode potential is stepped from the initial value $E_i = 0.13$ volts where Qu is electrochemically inactive, to a final value of $E_f = 0.49$ volts where the electrode reaction proceeds. The potential is held at E_f, for time τ after which it is stepped back to E_i and maintains there for the same time interval. On plotting $i(t > \tau)$ versus $t^{-1/2}$ for the first cv wave, straight regression lines are obtained with regression coefficients of 0.9994 for all used duration times, c.f. Fig. 3A. This reveals that the oxidation of quercetin is a diffusion-controlled process over the entire range of time. From the slope, the value of D is obtained. The mean value of D is estimated to be $2.26 \times 10^{-6}\ cm^2\ s^{-1}$.

3.3. Double potential step chronocoulometry

Double potential step chronocoulometry has found considerable use in the investigation of the adsorption of electroactive species. For chronocoulometric experiment, the electrode potential is stepped from initial value $E_i = 0.130$ volt to a final value of $E_f = 0.595$ volt. E_f is fixed for time τ after which it is stepped back to E_i and maintains there for the same time interval. The charge that passes through the electrode during each of the time intervals is measured. The charge of the electrode potential from E_i to a more positive value of E_f causes oxidation of both adsorbed and diffusing Qu. Upon reversing the potential step, the cathodic reaction proceeds, and the charge ratio, $Q(2\tau)_{red}/Q(\tau)_{ox}$, where $Q(2\tau)_{red}$ and $Q(\tau)_{ox}$ are the charge that passes through the electrode during the time intervals 2τ and τ, respectively, deviates from the expected theoretical value 0.586 (Abdel-Hamid, 1998). This is attributed to an irreversible consumption of the oxidized product generated at the forward step. In the double potential step chronocoulometry, electrochemical responses are given by Eqs. (2) and (3) for the forward and reverse steps, respectively (Abdel-Hamid, 1996).

$$Q(t < \tau) = \frac{2n\mathrm{FAD}^{1/2}\mathrm{C}^{*}_{\mathrm{bulk}}t^{1/2}}{\pi^{1/2}} \tag{2}$$

$$Q(t > \tau) = \frac{2n\mathrm{FAD}^{1/2}\mathrm{C}^{*}_{\mathrm{bulk}}}{\pi^{1/2}}[t^{1/2} - (t-\tau)^{1/2}] \tag{3}$$

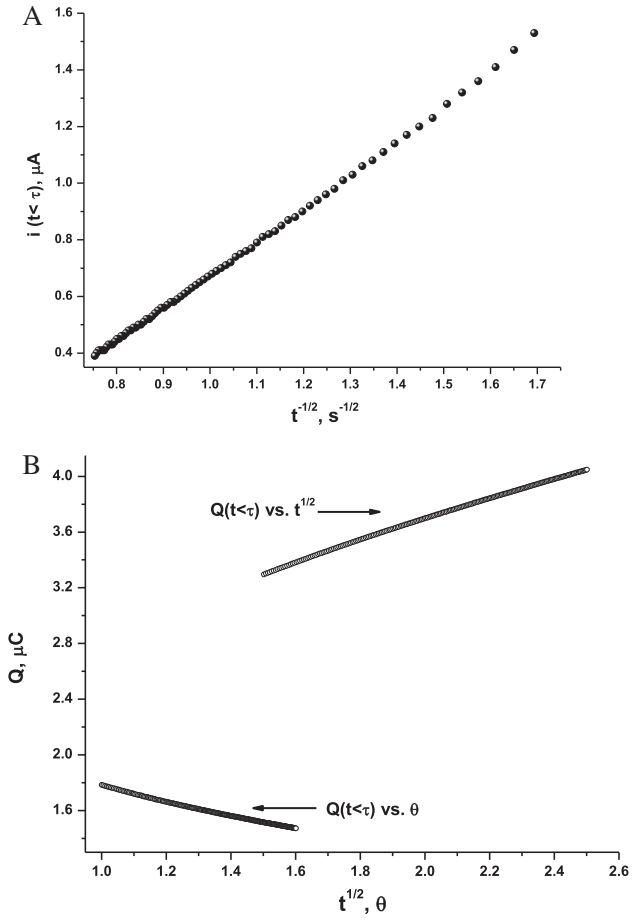

Figure 3 A $i(t < \tau)$ vs. $(t^{-1/2})$ relation of 2.5 μM Quercetin in 0.2 M phosphate buffer pH 2.12 at duration time of 10 s. B: Anson Plots of $Q(t > \tau)$ vs. $t^{1/2}$ and $Q(t < \tau)$ vs. θ for 2.5 μM Qu second wave.

where A is the electrode area, C^*_{bulk} the bulk concentration of analyte, D is the diffusion coefficient, t is the time and n and F have their usual meanings. When reactant adsorption occurs, additional terms was added to Eq. (2), where Γ is the amount of the adsorbed species and Q_{dl} is the charge of the double-layer.

$$Q(t < \tau) = \frac{2n\mathrm{FAD}^{1/2}\mathrm{C}^*_{bulk}t^{1/2}}{\pi^{1/2}} + Q_{dl} + \mathrm{nFA}\Gamma \quad (4)$$

Thus, from Eqs (3) and (4), $Q_T(t) = Q(\tau) - Q(t > \mathrm{t})$ can be expressed by Eq. (5).

$$Q_T(t) = \frac{2n\mathrm{FAD}^{1/2}\mathrm{C}^*_{bulk}}{\pi^{1/2}}\theta + Q_{dl} \quad (5)$$

where $\theta = (\tau^{1/2} + (\mathrm{t}-\tau)^{1/2} - \mathrm{t}^{1/2})$.

The first term of the right-hand side of Eq. (2), represents the charge of species that oxidize under diffusion-control. A straight line will be obtained on plotting $Q(t < t)$ against $t^{1/2}$ with an intercept equal to Q_{dl}. A separate experiment using the supporting electrolyte alone is carried out to measure the charge of the double-layer, Q_{dl}. On plotting $Q(t-\tau)$ against $t^{1/2}$ for the first cv wave, a straight regression line is obtained with regression coefficient of 0.999. This supports that first cv wave is diffusion-controlled. Moreover, the diffusion coefficient is determined to be 2.31 x 10^{-6} cm^2 s^{-1}.

Fig. 3B represents the plots of $Q_T(t)$ against θ and $Q(t < t)$ against $t^{1/2}$ for the second cv wave. Straight lines are obtained in the entire duration time range of investigation. It is clear that the intercept according to Eq. (5) is always less than that obtained for the $Q(t < t)$ against $t^{1/2}$ plots, Eq. (4). This further supports that Qu molecules adsorb on the surface of the working electrode. Furthermore, from the difference in the intercepts for the forward and reverse, Anson plots (Eqs. (4) and (5)), the amount of the adsorbed quercetin is estimated. The charge obtained for 2.5 μM quercetin is 0.80 μC/cm^2. This value is equivalent to a surface excess Γ_o of 1.002 x 10^{-10} mol/cm^2. The charge obtained for 2.5 μM quercetin is 0.80 μC/cm^2.

Although cyclic voltammetry is used in quantitative measurements, the complex nature of the electrode mechanisms limits its use in quantitative investigations of coupled chemical reactions. In comparison the double potential step chronocoulometry method is more suitable for such quantitative studies. The charge ratio, Eq. (6), is obtained from the ratio of Eq. (2) at $t = \tau$ and Eq. (3) at $t = 2\tau$.

$$Q_R = \frac{Q_b}{Q_f} = \left[\frac{Q(\tau) - Q(2\tau)}{Q(\tau)}\right] \quad (6)$$

The experiments are performed by varying the duration time, τ, over a suitable range and measuring the charge ratio Q_R. The experimental results are compared with the theoretical response ratio for various mechanisms in an attempt to find a satisfactory match. Chronocoulometric response ratios for 22 electrochemical mechanisms described by Hanafey et. al. are used for tracing the Qu oxidation mechanism (Hanafey et al., 1979). The experimental Q_R versus log τ plots is matching with the theoretical working curves that had been calculated for the different electrode mechanisms. The satisfactorily matching mechanism is found to be one of the three ECEC mechanisms, ECEC, radical–radical dimer, ECEC, parent-radical dimer and ECEC, first order. On matching the experimental and theoretical curves, an excellent fit is seen to be ECEC, first-order mechanism, c.f. Fig. 4.

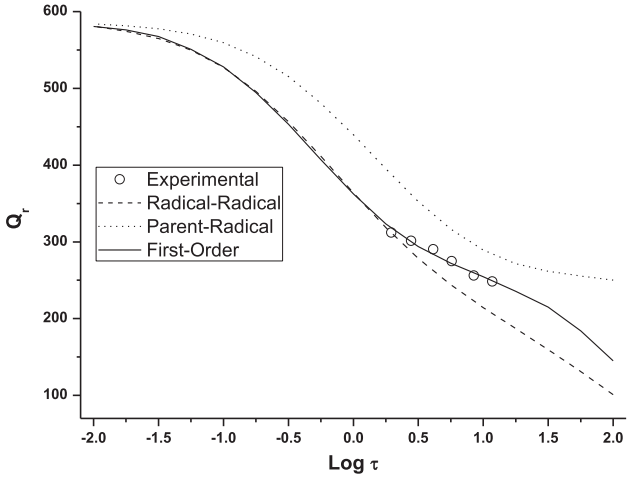

Figure 4 Best fit of chronocoulometric charge ratio, Q_R for experimental and theoretical working curves for the oxidation ECEC mechanisms of quercetin.

3.4. Digital simulation

The electrochemical oxidation of quercetin at pH 2.12 proceeds according to Scheme 1 according to the ECEC first-order mechanism. Digital simulation confirms the mechanism. Initial reversible electron transfer to the quercetin molecule, species Qu, gives the radical-cation, Qu^+. The standard potential E_1^o with a rate constant k_1^o assigns this redox couple. Neutral radical species, Qu•, forms on deprotonation of the radical cation in the first chemical step with a rate constant k_f^1. The neutral radical species (Qu) then undergoes further reversible electron transfer step with standard potential E_2^o to form the monocation Qu^+ with electron transfer rate constant k_2^o. The monocation Qu^+ will yield the final product QuO via a first-order deprotonation process with rate parameter k_f^2 following ECEC first-order mechanism.

$$Qu \overset{k_1^o}{\rightleftharpoons} Qu^{+\bullet} + e^-$$
$$Qu^{+\bullet} \overset{k_1^f}{\rightleftharpoons} Qu^{\bullet} + H^+$$
$$Qu^{\bullet} \overset{k_2^o}{\rightleftharpoons} Qu^{+} + e^-$$
$$Qu^{+} \overset{k_2^f}{\rightleftharpoons} QuO + H^+$$

Scheme 1

To establish the theoretical working curves, digital simulation of the proposed mechanism is carried out. The experimental voltammograms are compared with the theoretical ones calculated using the DigSim 3.03 software, in order to confirm the electrode mechanism and to estimate the kinetic parameters for the heterogeneous electron transfers and their associated chemical steps. For the diffusion coefficient, D, the default value of 2.26 x 10^{-6} cm^2/s^{-1} is used throughout.

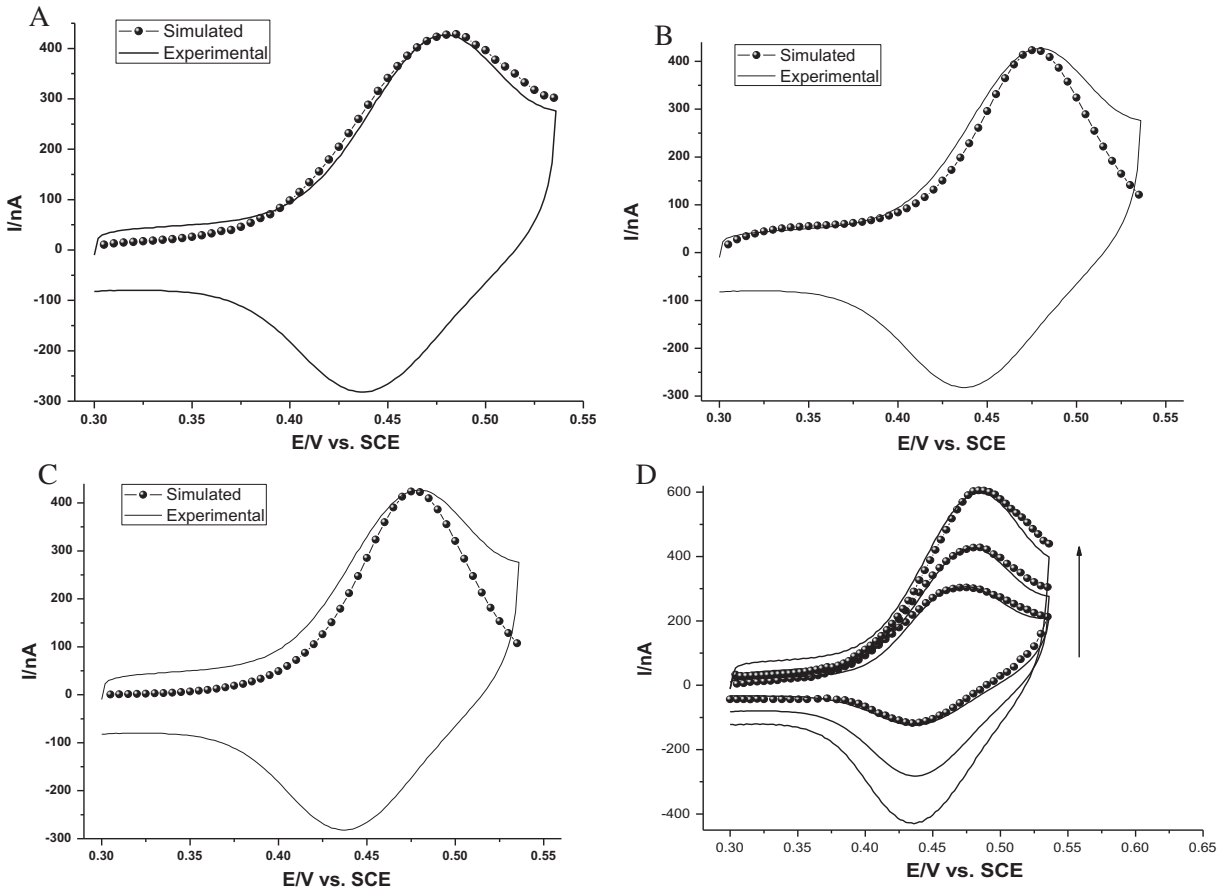

Figure 5 Experimental and digital simulated data for the quercetin oxidation mechanisms, (A) ECEC, first-order, (B) ECEC, radical–radical dimer and (C) ECEC, parent-radical dimer at pH 2.12 and scan rate of 20 mV/s, D- represents the fit cv for the ECEC, first-order at different scan rates, 10, 20 and 30 mV/s.

Table 1 Kinetic parameters for the electrochemical oxidation of 0.20 μM quercetin at pH 2.12 and a scan rate of 20 mV s^{-1}.

E_1^o/mV	E_2^o/mV	k_1^o/cm s^{-1}	k_2^o/cm s^{-1}	K_1^c/s^{-1}0.25		K_2^c/s^{-1}1.00	
				$k_f^1 \times 10^5$	$k_b^1 \times 10^5$	$k_f^2 x 10^6$	$k_b^2 \times 10^6$
455	200	0.50	0.10	1.530	6.104	4.001	4.003

Different ECEC mechanisms including ECEC radical–radical dimmer; ECEC parent–radical dimmer, and ECEC first-order are tested. The transfer coefficient, α, is assumed to be 0.5, and the formal potential E_1 is obtained experimentally from the first cv wave observed in cyclic voltammetry and E_2 has a value more or less of E_1.

Fig. 5 represents the matching voltammograms of the simulated and experimental results for the different electrode ECEC mechanisms proposed for quercetin oxidation at pH 2.12. Good agreement between simulated and experimental voltammograms is obtained for the ECEC first-order mechanism. Fig. 5D represents the simulated and experimental voltammograms obtained for the ECEC first-order mechanism at different scan rates. Table 1 depicts the kinetic parameters obtained for the best fit. Thus, the simulation using the proposed ECEC first-order mechanism, c.f. Scheme 1, agrees well with the experimental data.

4. Conclusion

The electrochemical oxidation of quercetin proceeds by a consecutive mechanism and is related with the catechol groups in ring B and the three hydroxyl groups in A and C rings. The oxidation of the catechol moiety occurs first at low positive potentials and corresponds to two electron and two proton reactions following the ECEC first-order electrode mechanism. The two chemical steps, C, are deprotonation, since the peak potential is shifted to less positive values and the peak current decreases on increasing the pH of solution. Quercetin is strongly adsorbed on the electrode surface.

References

Abdel-Hamid, R., Newair, E., 2011. J. Electranal. Chem. 657, 107.

Abdel-Hamid, R., 1998. Monatsh. Chim. 129, 817, and the references therein.

Abdel-Hamid, R., 1996. J. Chem. Soc. Perkin Trans. 2, 691.

Álvarez-Diduk, R., Ramírez-Silvaa, M.T., Alarcón-Ángelesa, G., Galanoa, A., Rojas-Hernándeza, A., Romero-Romob, M., Palomar-Pardavé, M., 2009. ECS Transactions 20, 115.

Bard, A.J., Faulkner, L.R., 2001. Electrochem. Methods. In: Fundam. Appl.. Wiley, New York, 2nd ed.

Brett, A.M.O., Ghica, M-E., 2003a. Electroanalysis 15, 1745.

Brett, A.M.O., Ghica, M-E., 2003b. Electroanalysis 15, 1736.

Gutiérrez, F., Ortega, G., Cabrera, J.L., Rubianes, M.D., Rivas, G.A., 2010. Electroanalysis 22, 2650.

Hanafey, M.K., Scott, R.L., Ridgway, T.H., Relley, C.N., 1979. Anal. Chem. 50, 116.

He, J-Bo., YU, C-Li., Duan, Ti-Lan., Deng, N., 2009. Anal. Sci. 25, 373.

Jin, G-P., He, J-Bo., Rui, Ze-Bao., Meng, Fan-Shun., 2006. Electrochim. Acta 51, 4341.

Manach, C., Scalbert, A., Morand, C., Remesy, C., Jimenez, L., 2004. Am. J. Clin. Nutr. 279, 727.

Mase, A., Zaborski, M., Chrzescijanska, E., 2011. Food Chem. 127, 699.

Medvidović-Kosanović, M., Šeruga, L., Jakobek, M., Novak, I., 2010. Croat. Chem. Acta 83, 197.

Mora, A., Paya, M., Rios, J.L., Alcaraz, M.J., 1990. Biochem. Pharmacol. 40, 793.

Mulazimoglu, I-M., Ozkan, E., 2008. E-J. Chem. 5, 539.

Nematollahi, D., Malakzadeh, M., 2003. J. Electroanal. Chem. 547, 191.

Pierozynski, B., Zielinska, D., 2011. J. Electroanal. Chem. 651, 100.

Pierozynski, B., Zielinska, D., 2010. Int. J. Electrochem. Sci. 5, 1507.

Simić, A., Manojlović, D., Šegan, D., Todorović, M., 2007. Molecules 12, 2327.

Timbola, A.K., de Souza, C.D., Giacomelli, C., Spinelli, A., 2006. J. Braz. Chem. Soc. 17, 139.

van Acker, S.A.B.E., van den Berg, M.N.J.L., Griffioen, D.H., van Bennekom, W.P., van der Vijgh, W.J.F.A., 1996. Bast free radic. Boil. Med. 20, 331.

Yang, B., Aral, K., Kusu, F., 2001. Anal. Sci. 17, 987.

Zare, H.R., Namazian, M., Nasirizadeh, N., 2005. J. Electroanal. Chem. 584, 77.

Zielinska, D., Pierozynski, B., Wiczkowski, W., 2010. J. Electroanal. Chem. 640, 23.

Zielinska, D., Pierozynski, B., 2009. J. Electroanal. Chem. 625, 149.